Renewable Energy 164 (2021) 1230–1243

Contents lists available at ScienceDirect

Renewable Energy

journal homepage: www.elsevier.com/locate/renene

Development of an irradiance-based weather derivative to hedge cloud risk for solar energy systems

Colin F.H. Boyle [a], Jannik Haas [a, b, *], Jordan D. Kern [c]

[a] Department of Stochastic Simulation and Safety Research for Hydrosystems (IWS/SC SimTech), University of Stuttgart, Germany
[b] Department of Energy Systems Analysis, Institute of Networked Energy Systems, German Aerospace Center (DLR), Stuttgart, Germany
[c] Department of Forestry and Environmental Resources, North Carolina State University, Raleigh, NC, 27695, United States

ARTICLE INFO

Article history:
Received 9 July 2020
Received in revised form
19 October 2020
Accepted 21 October 2020
Available online 27 October 2020

Keywords:
Weather derivative
Weather risk
solar photovoltaic and battery storage systems (PV BESS)
Energy system planning
System optimization

ABSTRACT

For large energy consumers transitioning to high shares of solar energy, irradiance variability causes volatility in power generation and energy expenditures. Volatility in an end user's cash flow is harmful to their financial health, especially in abnormally cloudy years. This paper explores the utility of an irradiance-based weather derivative in mitigating cloud weather risk and measures the effectiveness of the developed derivative by applying it to a case study of two Chilean copper mines. Weather derivatives are financial instruments tied to an underlying weather variable that act as an insurance for the contract holder, executing indemnity payments based on an index value. This research develops a contract with a combined index based on monthly sums of irradiance and cloudy day sequencing to mitigate a solar mine's weather risk. The design and evaluation of contracts are based on LEELO, a linear optimization model outputting optimal sizes of solar photovoltaic, battery storage, and power-to-gas systems, as well as the operation of these systems for a given mine's load, irradiance and technology costs. Results indicate contracts are effective in cloudier climates with increasing utility for mines installing solar energy systems until the year 2030. After 2030 batteries begin to become a more cost-effective risk-hedging mechanism as they become more affordable.

1. Introduction

Weather risk remains a major influence in our economy, affecting firm cash flows in various sectors from energy and agriculture to construction and tourism. To combat this risk, traditional indemnity insurance has been the leading method for reimbursing loss due to adverse weather, and has typically addressed catastrophic events (e.g. flooding, hurricanes). Weather risk will only increase as climate change triggers growth in weather volatility [1]. In the last 20 years, index-based financial instruments have seen a large uptake in use as a financial/actuarial tool to curb exposure to weather hazards and increase company value while also streamlining the insurance process for both insured and insuring parties [2]. Weather-based indexed financial instruments, also known as weather derivatives, have also been viewed as a strong alternative to traditional insurance as they better address end users who experience a higher frequency of non-catastrophic weather risk while covering those who experience low frequency high magnitude events [3]. In the renewable energy sector, weather plays an influential role affecting both energy demand *and* production. The use of weather derivatives to curb weather risk in the renewable energy industry can lead to more stable cash flows for renewable energy producers and increase their ability to attract investors.

Weather derivatives may also mitigate weather risk for large energy end-users adopting large shares of renewably produced energy, for instance industries installing commercial-scale solar arrays to power their operations. Distributed commercial and industrial solar PV capacity is forecast to expand from 150 GW in 2018 to 377 GW in 2024 [4], making this sector a crucial element in the transition to a green energy matrix.

Energy system modeling and planning has traditionally addressed energy storage as the default method of managing uncertainty in renewable energy systems. Future energy storage requirements have been synthesized in Refs. [5]. Planning approaches and trends for such energy systems have been addressed in Refs. [6]. From these reviews, it is clear that managing solar generation risks with financial instruments is not widely used thus far.

* Corresponding author. Department of Stochastic Simulation and Safety Research for Hydrosystems (IWS/SC SimTech), University of Stuttgart, Germany.
E-mail address: Jannik.Haas@iws.uni-stuttgart.de (J. Haas).

https://doi.org/10.1016/j.renene.2020.10.091
0960-1481/

This paper focuses on the development of a weather derivative with an index based on irradiance with the purpose of mitigating cloudy day weather risk for commercial PV solar installations. The derivative is meant to act as an insurance that awards payments to the contract holder (a commercial entity that is producing their own on-site power via PV) when there are above average cloudy days and reduced PV power generation. The goal is to achieve reduced volatility in the contract holder's cash flow that may result from exceptional energy expenditures during cloudy (low solar generation) periods when the contract holder must purchase additional energy from another source (such as the grid), potentially also incurring penalties for violating energy/power contracts.

The weather derivative in this study is developed and evaluated in the context where the contract holder is a Chilean mine. This context is chosen because mining is a core pillar of Chile's economy, accounting for nearly 10% of GDP in 2019 [7], and it is an energy intensive sector. The country also receives some of the highest amounts of irradiance in the world, especially in its northern Atacama region, making it a perfect candidate for solar projects. Already mines in Chile have begun installing their own industrial sized PV plants to supplement their energy needs, such as mining company Anglo American's 86 kW floating solar array, installed on one of its tailing ponds [8].

Previous literature addressing solar risk and weather derivative contracts exists, though to a very limited extent and addresses generators not end users. Thus, the objectives of this study are:

1. Develop an irradiance-based index and weather derivative contract to reduce the financial risk in energy end-user systems with high solar shares.
2. Evaluate the derivative's effectiveness for:
   - Two different climates where the contract is applied.
   - Different points in the future with declining solar and battery technology costs.

A successful contract will help stabilize the mine's finances and can potentially be applied in other industries looking to transition to solar autonomy that might be wary of financial volatility.

To lay the foundation for the development of these contracts, the remainder of this paper is divided into four further sections: (2) A brief review of weather derivatives, (3) a methods section broken into separate parts for identifying the underlying index, structuring the contracts, pricing the premiums, and laying the framework for their evaluation, (4) a results and discussion section summarizing the outcome of the developed indices and contract evaluation, and (5) a conclusion summarizing the findings of this paper.

2. Review of weather derivatives

Index-based contracts determine payouts based on a certain metric or "index", which can range from stock and commodity prices to currency [9]. Financial instruments that use weather-based indices (e.g. temperature, rainfall, or wind speed) act to hedge financial risk correlated with the respective weather index. As opposed to traditional derivatives that hedge "price" risk, or risk that is associated with the price volatility of the asset or index, weather derivatives can address "volumetric" risk and hedge risk correlated to the quantity of the index [10]. These contracts can come in the forms of futures, forwards, options and swaps, and trigger payments based on the value of the index at the end of the contract period [11]. These payments act as compensation for any financial loss the contract holding party might have suffered due to the index hitting a predetermined index value (called a "strike").

Weather derivatives were first developed in 1997 by energy companies as a way to hedge weather risk, defined as "uncertainty in cash flows and earnings caused by non-catastrophic weather events" [12]. Following the privatization of the U.S. electricity industry, drops in sales resulting from a decrease in consumption due to warm winters or cool summers could no longer be made good by price increases, therefore temperature-based indices using cooling and heating degree days began to receive a great deal of attention [9]. For instance, a utility could buy a temperature-based contract to hedge any loss that might occur during a mild summer when air conditioning use (and hence energy consumption) is reduced. This contract would reduce the utility's losses by awarding payouts commensurate to the loss the utility experienced from the decrease in electricity sales.

In the food and beverage sector, weather has a significant influence on the purchasing behavior of shoppers. In Ref. [13], temperature was shown to have a statistically significant effect on beverage sales in 60 large food stores in Croatia and weather derivatives proved to be effective in beverage sales uncertainty reduction.

Attention has also been put toward precipitation-based contracts due to the influence of rainfall in various industries [14]. In the agricultural sector there exists various rainfall and temperature-rainfall-based derivatives. In Serbia [15], the sum of monthly precipitation from April–May was used to determine payouts to wheat farmers and the sum of monthly precipitation from April–August to determine payouts to corn farmers. Results of this study showed a decrease in standard deviation in revenues of the farmers by 21% in the case of wheat and 18% in the case of corn.

In [16], the efficiency of weather derivatives as a primary insurance instrument was analyzed for six crop reporting districts that are among the largest producers of corn, cotton, and soybeans in the United States. The efficacy of the derivative contracts varied by crop and region, and the indices were composed of functions with inputs of both temperature and rainfall for certain months of the growing season. Results showed significant reductions in risk as measured by Mean Root Square Loss (MRSL) and Value-at-Risk (VaR) in $/acre for certain crops while other crops actually performed better without the contracts.

In wind energy, parameters such as wind speed, wind direction and wind duration play a critical role in power generation and have been used as parameters for derivative indices. In Ref. [17], the pricing equations for wind futures is written on two indices, the cumulative average wind speed index and the Nordix wind speed index. In 2019, Enel Green Power began construction of the High Lonesome wind farm project, the largest wind farm in its portfolio in the US, hedging 295 MW of the total 450 MW capacity with a long-term proxy revenue swap based on wind speed [18].

In [19], irradiance is inputted as a parameter to a solar energy generation model for a generator using natural gas as a generation backup- back-up generation source with models for natural gas price, solar power production, energy demand and energy price. It was observed that there was little variation in the generator's profit during peak summer months when there is little solar variability and there are high electricity prices. On the contrary, fringe summer months and winter months showed high cash flow variance. To hedge the increased risk in these months, an explicit cross-hedge was performed via call and put options using cooling and heating degree days. It was concluded that these contracts effectively reduced the profit variation risk of the generator in the risk-prone months. In Ref. [20], a derivative was developed based on solar prediction error. This study was aimed toward solar generators whose reliance on the prediction of future solar conditions is important for the quotation of day-ahead sales contracts and preparation of alternative fuel sources to meet demand.

The value of purchasing a contract depends on the risk exposure of the potential contract buyer and what their specific firm goals

may be. In certain cases, exposure to weather risk can cause financial ruin or bankruptcy, in the instance of farmers who might be operating with high amounts of debt and cannot meet credit repayments because of poor yields due to drought or extreme temperature in a given year [21]. The same can be said of power producers who may have substantial portions of hydro generation within their portfolios and thus are exposed to a great amount of hydrologic risk. In Refs. [22], index-based financial instruments were applied to the hydrologic risk of a hydropower producer and incoming reservoir stream flow was used as an underlying index. Evaluation of the contract was done by comparing the insured and non-insured "revenue floors" of the generator, i.e. the minimum revenues experienced by the generator during dry years with and without the contract. In the study, it was shown that the generator could significantly reduce losses during these dry years at a low opportunity cost (< 3% total revenues).

Contract buyers may also be interested in reducing the volatility in their cash flows since this improves their credit rating and rates of borrowing capital [3]. A greater volatility can also lead to additional financial burdens such as taxes, external financing costs, and higher under-investment costs. The most common measure of volatility in cash flow is standard deviation, though it is argued that semi-deviation (below-mean deviations), is a better metric as investors are only concerned by negative deviations [3]. The use of value-at-risk (VaR) for comparing revenues of corn producers in Switzerland with and without weather derivatives has also been used and deemed a feasible, yet less common, way to evaluate the value of a contract [23].

3. Methods

This study utilizes an existing linear optimization model called LEELO [24] that] minimizes the total energy expenditure of a system. In this paper, a simplier instance of LEELO is used, as shown in [25,26], which will be referred to as the mine energy management model. The model acts by minimizing operational and investment costs of the energy system by inputting solar irradiance and energy demand and outputting the sizes of a solar photovoltaic (PV), battery energy storage system (BESS), and power-to-gas system along with an optimal contract size and energy import/export operation schedule. In terms of the power-to-gas systems, we assumed that after the electrolysis methanation follows, to use the resulting methane at later times with a gas turbine (for more information, see Ref. [27]).

Weather derivatives are designed based on historical data, correlating a firm's financial well-being with a spatially-explicit weather process (e.g. irradiance), with contract parameters optimized within the context of the mine's operation described above. The weather derivative aims to reduce expenditures for cloudier, higher-cost years when the PV system generates less power and the mine's grid energy imports increase. This weather derivative can reduce the variation in the mine's variable costs together with the photovoltaic battery energy storage system (PV-BESS). The modeled mine's energy demand profile is based on the semi-autogenous grinding (SAG) mill, the component of a mine that breaks down ore for further processing and which is responsible for roughly 50% of a typical mine's energy consumption.

3.1. Model details and case study simulation

The model inputs consist of hourly mine load values and available PV profiles. Fixed inputs include grid energy import and export prices [€/MWh], power contract prices [€/MW], power contract exceedance penalties [€/MW], and costs for the PV-BESS and power-to-gas technologies. Costs for the different technologies are projected for the years 2020, 2025, 2030, 2035, 2040, 2045, and 2050 [28] (PV-BESS and power-to-gas systems will be referred to as the "energy system" in this paper). Fig. 1 shows the energy balance of the SAG model.

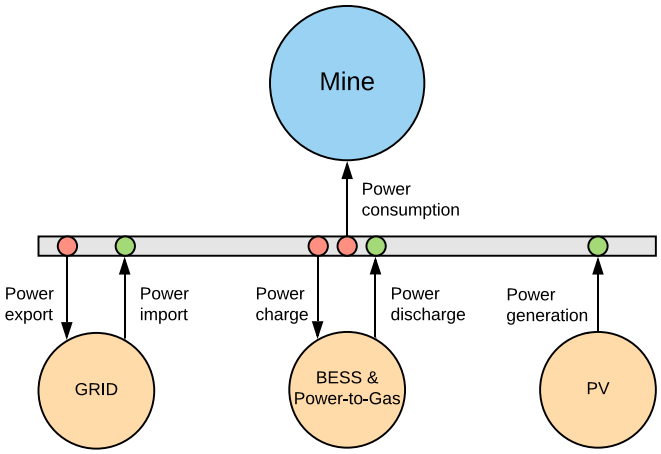

Fig. 1. Energy balance of mine energy management model.

In this study, randomly simulated years of hourly mine load and PV profiles were generated using the mining and solar models to parameterize and evaluate the derivative contracts. Details of the mining model are explained in Ref. [26].

Solar PV input was generated using a solar model, which uses Markov Chains to randomly generate PV profiles based on historic irradiance data [25]. Historical irradiance time series are obtained from *Explorador Solar*, a project developed by the geophysics department at the University of Chile in conjunction with the Chilean Ministry of Energy [29]. *Explorador Solar* incorporates a model for PV power plants, allowing users to dictate the specifications of their PV system, and which in turn generates PV power production at an hourly resolution in tandem with irradiance values.

Chile is a climatically diverse country, with an arid desert climate in the north and Mediterranean climate to the south. Mining operations make up the majority of economic activity in the northern part of the country and are heavily centered about the Atacama Desert, where irradiance levels are some of the highest in the world. Mining also plays an important role in the mid and southern parts of the country, which experience cooler climates and more overcast skies. Thus, to better understand a derivative's hedging ability, solar irradiance and PV profiles were generated for two different climatic regions (location 1 - Arid Atacama Desert, location 2 - Mediterranean Central Chile) sharing large portions of mining activity.[1] The PV base profiles were then multiplied by the size of the PV plant (determined as part of the optimization) which produced generated energy for that hour.

400 random years of solar profiles were generated for each location and inputted into the energy model. The model was then run with the generated profiles in both locations for the years 2020, 2025, 2030, 2035, 2040, 2045, and 2050 (these years will be further

[1] For the input to the *Explorador Solar* PV model, a single axis inclined E-W tracker was selected for both locations. The inclination angle for each location was then optimized to produce the greatest average hourly amount of yearly PV as possible (17° for location 1, 20° for location 2). An inverter efficiency of 98%, plant energy losses of 10%, and a temperature coefficient of −0.5%/°C were selected for both locations. The total installed capacity of the plant was selected to be 1 kW, resulting in normalized base profiles whose amplification within the optimization corresponds to a 1 MWp (Mega Watt peak, which is the maximum of the plant).

referenced as "milestone" years to avoid confusion with the generated solar profile years), while keeping the generated demand profiles between the locations constant. The result of this were 400 distinct output sets (energy system sizing, contract size, total annual energy cost, etc.). From each output set the total annual energy expenditure was taken, making a series of 400 data points of total energy costs. The derivative contracts were then designed based on the first 300 data points of this data series by correlating each point with its respective solar irradiance inputs, and the remaining 100 data points were used for evaluating the contracts (Fig. 2). Thus, one can see the effectiveness of the contracts on a spatial and temporal basis.

3.2. Contract modeling

Index-based contracts require four key components [30]:

1. A measurable and transparent metric (i.e. index) that corresponds with financial loss of the contract holder
2. A contract period/length
3. A structure that describes the conditions of the index, the size of payments, and how payments should be made (called the "payout function")
4. A contract premium

These four components will be explored next.

3.2.1. Identifying underlying index

Index-based contracts are often advantageous over traditional casualty insurance as payment timing and payment size are index-dependent, therefore the insurer must simply determine the index value at the end of the contract period and plug it into the payout function. There is no need for a subjective assessment of damages, which reduces administrative costs, as well as a reduction in "moral hazard", which is the risk that the contract holder might manipulate their financial loss and commit insurance fraud (e.g. damage untruthfully or incorrectly attributed to an insured risk) [31].

There does, however, remain a certain amount of "basis risk" within index-based contracts, which occurs when there is an imperfect correlation between the index and the actual financial loss [32]. Past literature has used the coefficient of determination (R^2) between the index and financial metric the index wishes to predict as the primary determinant of index quality and relative basis risk.

Lower basis risk cases have been seen in weather derivative contracts designed for hydropower generators, where incoming reservoir streamflow is used as an index. In these circumstances the R^2 value between stream flow and company revenues measured to be between 0.85 and 0.96, depending on the season [22]. Correlations have also been much smaller, particularly in agriculture, where crop yields are determined by a plethora of factors. In Ref. [16], compound indices made using regressions based on rainfall and temperature of specific months of the growing season for various crop groups in different regions of the US resulted in R^2 values ranging from 0.36 in Illinois for soybeans to 0.87 for corn in the same region. In Ref. [33], linear regressions using temperature and rainfall for the months June–August were developed to predict crop yield for corn, soybeans and hay in Ontario, Canada. The R^2 values obtained for the respective crops were 0.33, 0.27 and 0.31. Thus the predictive ability of the index in the cases studied show a large range of variability.

In the case of the energy system optimization model, the goal is to correlate the index with total annual energy cost (expenditure inlcuding investment costs). The underlying used to design the index is global irradiance measured on an inclined surface with tracking, which can be implemented in practice by installing a pyranometer along side the PV panels or a meteorologic station nearby.

The two predominant factors affecting the mine's operational costs are total energy imports and contract exceedance penalties. Total energy imports have a strong negative correlation to annual, and even more so monthly, sums of irradiance. Contract penalties are significantly more difficult to predict and are not correlated to the same degree with monthly radiation as are general energy imports. How contract penalties work is that at the end of the year, the mine must pay a certain sum per every MW of power exceeding

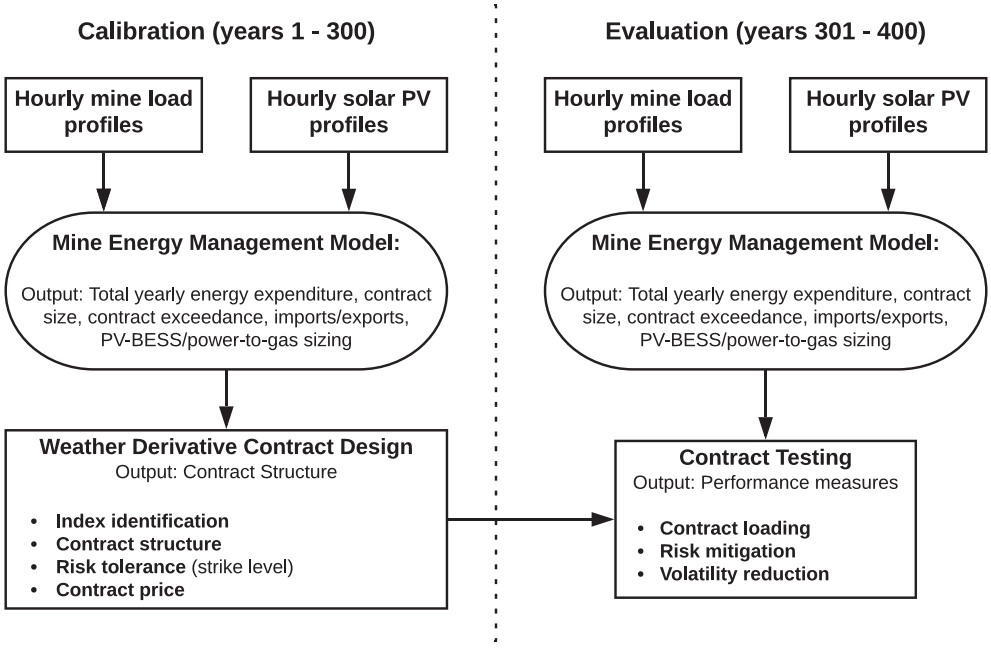

Fig. 2. Schematic of framework used in this study.

their power contract. For example, if the mine exceeded its contract by 1, 2, and 3 MW at three different times throughout the year, it would pay the maximum of these exceedance instances, 3 MW, by a penalty rate, €/MW, defined a priori. These penalties are generally triggered when sequences of poor irradiance days (i.e. cloudy days) occur. This suggests that classifying cloudy days is necessary to developing a strong index.

To have a better understanding of the distribution of cloudy days for locations 1 and 2, their hourly irradiance profiles are summed into daily quantities, then each day is transformed to a percentage of the clear-sky maximum possible sunshine for that day. When comparing the distributions of days as percentages of their daily maximum value, there are stark contrasts between locations 1 and 2 (Fig. 3). Location 1, located in the sunny Atacama Desert, has a minimal amount of days that drop below 60% of the clear sky maximum, while nearly half of days fall below 80% of a clear sky at location 2. In the results section, it is shown that very low irradiance days have a strong negative correlation to energy cost spikes. The percentage range of these exceptionally cloudy days is determined by analyzing which percent ranges triggered higher than normal grid energy imports and power contract exceedances on a daily resolution. This is done for both locations and these very poor ranges are termed "Bad" cloudy days. Three more ranges were then declared based on their frequencies as seen in Fig. 3, "Moderate" and "Good" cloudy days making up the bulk of days seen during the year, and then an "Excellent" cloudy day class, making up the smaller percentage of nearly clear sky days. The break down of these classes for each location is given in Table 1.

To develop the index as a reliable predictor of total energy cost, multiple linear regressions were performed for both locations and for each milestone year modeled using the 300 years of generated annual energy costs and their relative values of monthly sum irradiance and yearly total counts of the sequences of each sunshine class. Thus each location and milestone year obtained an index, *S*, in the form of the following regression:

Table 1
Definition of cloudy day classes based on percent ranges of clear sky maximum.

Class	Location 1	Location 2
Bad	0–60%	0–30%
Moderate	60–85%	30–80%
Good	85–95%	80–95%
Excellent	95–100%	95–100%

$$S = C_o + C_1 I_{Jan} + \ldots + C_{12} I_{Dec} + C_{Bad1} Bad_1 + \ldots + C_{Badn} Bad_n + C_{Mod1} Mod_1 + \ldots + C_{Modn} Mod_n + C_{Good1} Good_1 + \ldots + C_{Goodn} Good_n + C_{Exc1} Exc_1 + \ldots + C_{Excn} Exc_n \quad (1)$$

where C_o is an intercept, I values are individual monthly total sums of irradiance and $C_1 \ldots C_{12}$ are their respective coefficients. $Bad_1 \ldots Bad_n$, $Mod_1 \ldots Mod_n$, $Good_1 \ldots Good_n$, and $Exc_1 \ldots Exc_n$ correspond to the *yearly* total of cloudy day sequences according to the cloudy day class, where the sequence day length is denoted by the subscript. E.g Bad_3 would equal 5 if there were 5 counts of 3-day "Bad" cloudy day sequences in the year. C_{Bad1}, C_{Good1}, etc., are the corresponding coefficients to each yearly cloudy day sequence count.

For each location and milestone year, all variables shown in Equation (1) were shuffled and tested to see which indicators resulted in regressions with the greatest adjusted R^2 and significance (coefficient p-values < 0.05). The most influential variables were retained in the final selected regressions for index *S* and are reported in the results section.

3.2.2. Contract timing

Contracts are written on an "execution date", when the premium for the contract is paid. This occurs at some time before the

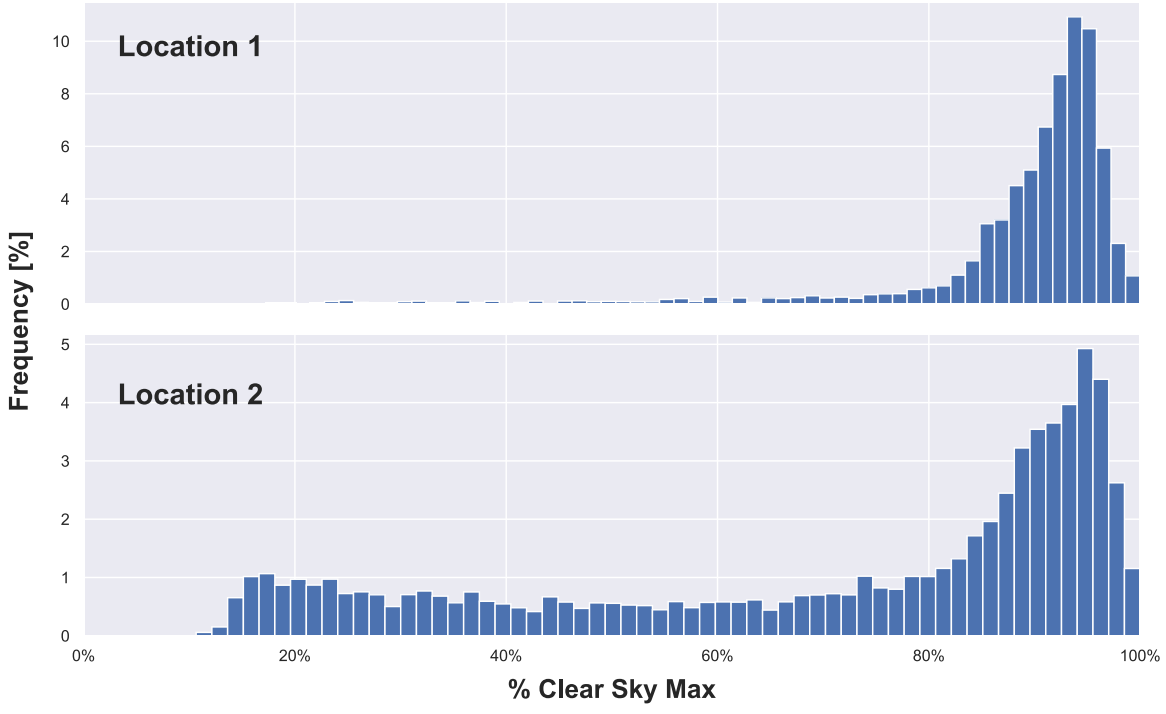

Fig. 3. Distribution of days as percent of clear sky maximum.

contract goes into effect, which is the "effective date", when the underlying of the index begins to be measured. Contracts then end on a "maturity date", when the final index is evaluated and payments are made based on the payout function [22].

Contract premiums are based on the historic probability of the index and the corresponding expected payout. If, at the time of the execution date, either party involved in the contract can predict the state of the index at the time of the effective date, the probability distribution of payouts needs to be adjusted. In the case of this study, we are assuming the simulated probability of payouts is equivalent to the historic probability of payouts and that at the time of the execution date, neither party can predict the state of the index at the effective date. Previous literature has used autocorrelation of the index being measured to determine buffer periods between execution dates and effective dates [22], so the same method is applied in this paper. Daily irradiance levels as percent of clear sky show statistically significant levels of autocorrelation (5%) out to 68 days, therefore requiring contracts to be written at least 68 days prior to their effective date (Fig. 4). Since contract exceedance penalties are paid annually, the period for the contract is one year.

3.2.3. Contract payout structure

Weather derivatives can take on a wide variety of different structures depending on the index being measured and goal of the contract [34]. A common derivative structure is an option, which can take the form of a "put" or "call", and behaves by calculating payouts in a linear fashion relating expected loss with change in the index value. Since the index in question predicts the mine's total energy cost, it is in the interest of the mine to hedge higher total costs. To do this, the mine will need to purchase a call option which triggers payments for higher index values. The structure of payouts, called the payout function, is described by

$$Payout(S) = A*MAX((S-K),0) \tag{2}$$

where S is the value of the index at the end of the contract period (millions €), A is the slope of the payout function, and K is the strike value (millions €), the index value at which payouts are initiated.

Values for the strike can differ and depend on how much coverage the insured party desires. The slope of the payout function can be determined in various ways, the most straight forward being the linear slope between the index being measured and the cost it is predicting. In the case of this paper, the index predicts total energy costs, thus the slope of the payout function is expressed as

$$A = \frac{\sum_{t=1}^{n} TotalCosts(t)}{\sum_{t=1}^{n} Index(t)} \tag{3}$$

where $TotalCosts(t)$ are the total costs for a given year t, $Index(t)$ is the index for a given year t, and n is the total amount of years.

It is important to note that the payout function does not include the premium paid by the contract buyer, which shifts down the payout function and is denoted by the dashed line in Fig. 5. This dashed line is called the "profit function".

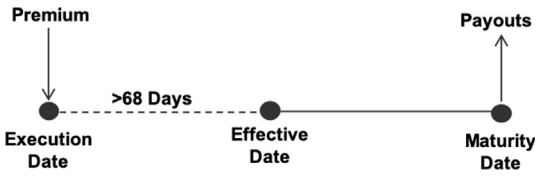

Fig. 4. Contract timing.

3.2.4. Contract pricing

Pricing weather derivatives poses certain challenges due to these contracts being relatively new and that they revolve around a non-tradeable index (irradiance cannot be traded). Since irradiance (and weather in general) is location dependent, these contracts are bought and sold on incomplete markets generally via over-the-counter (transactions between two private parties) and thus the "no arbitrage" principle cannot be used. This prevents common financial pricing methods, such as the Black-Scholes model, from being applied [35].

There do exist actuarial methods for pricing weather indexed derivatives, which set the "actuarially-fair" premium equal to the expected value of the payout function. This, however, does not take into account a "loading", which the writer of the contract adds to the option premium. This loading accounts for operational costs the underwriter might experience, expected profits, and "risk-loading". The risk loading refers to the additional risk the insurer is taking on given the fact that it may have to award substantially large payouts in the future and thus must set aside adequate liquid reserves, drawing opportunity costs. Contracts with more variable payouts, especially those with low probability - high magnitude events, will have higher risk-loading due to the insurer having to set aside seldomly used large sums of liquid reserves [36].

The method used in this study for the option pricing is the Wang Transform [37], which takes economic, financial and actuarial pricing theories and combines them to make a universal pricing method for financial and insurance risks. This method allows for pricing both traded and non-traded assets and liabilities, and acts by distorting the original payout probability distribution function by more heavily weighting its tails. The Wang Transform is given by the following equation:

$$F^*(x) = \Phi\left[\Phi^{-1}(F(x)) + \lambda\right] \tag{4}$$

where $F(x)$ is the original cumulative distribution function of payouts x, Φ is the standard normal cumulative distribution, λ is the "market price of risk", and $F^*(x)$ is the resulting "risk adjusted" cumulative distribution function of payments.

The "market price of risk", alternatively known as the Sharpe ratio, is a measure of the performance of an investment and is the ratio of the amount of return one would receive per unit of risk invested. This value is determined by evaluating existing market data, which in the case of weather derivatives is scarce as they are generally not publicly traded contracts. Therefore, following what has been done in previous studies [22,38], a λ value of -0.25 is used to calculate all risk adjusted premiums in this research (a negative

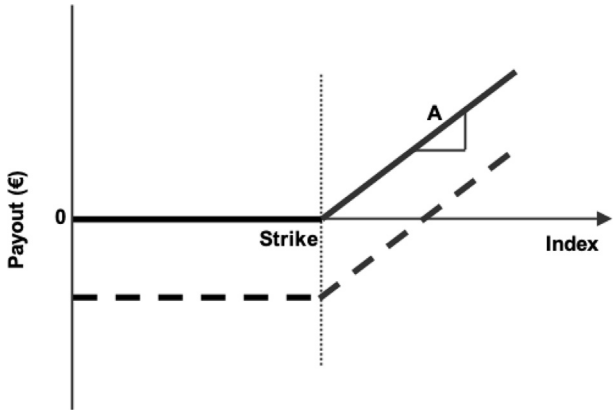

Fig. 5. Payout function.

value is chosen in order to generate a positive risk premium).

To utilize Equation (4) and determine the option premium, a number of methods used to price actuarial risks exist [36]. The most common and straight-forward is a "burn analysis", which uses historic data to calculate what payouts would have been with a contract in place and uses the distribution of historic data to calculate the price. Hence, after applying the transform, the premium is equal to the expected value of adjusted payouts, given by

$$Premium(x) = \sum[x * F^*(x)] \tag{5}$$

where $Premium(x)$ is the price of the contract.

A second method, "index modeling", is also commonly used and generally accepted to produce more accurate risk premiums. It is quite similar to the "burn analysis" as it takes the average of a series of payouts with a contract in place, though instead of using historic data (which may be minimal) to calculate the payouts, simulated payouts are used. This is done by fitting a distribution to historic index values and then preforming a Monte Carlo simulation by randomly generating indices from the fitted distribution and plugging them into the payout function. In our case, our historic indices are the 300 generated indices S, made using the respective regression equations formulated using 1. The generated payouts are given by

$$g(S(t)) = A*MAX((S(t) - K), 0) \tag{6}$$

where $g(S(t))$ is the payout and $S(t)$ is a randomly generated spot index taken from the index distribution. The premium is then calculated as

$$Premium(g(S(t))) = \sum[g(S(t))*F^*(g(S(t)))] \tag{7}$$

where $Premium(g(S(t)))$ is the price of the contract based on generated spot indices. Since index modeling is considered a superior method to option pricing than the standard burn method, various distributions were fit to the 300 generated indices for each milestone year and location, and the distributions that resulted in the best goodness of fit subject to the ranked average of the Kolmogorov Smirnov, Anderson Darling, and Chi-Squared tests were chosen for simulating more indices. Equation (7) was then applied using the generated indices.

The total energy expenditure for a given year with the contract is then given by

$$TotalCostsInsured = TotalCosts - Payout(K) + Premium(K) \tag{8}$$

where $TotalCosts$ are the costs without the contract and $Payout(K)$ and $Premium(K)$ are the contract payout and price given a certain strike K.

To analyze the cost of each contract from the perspective of the contract buyer, cost is depicted as the percent increase in total costs between the average total cost of the evaluation years and the average total cost of those years with the contract. This is then applied to various contracts with different strike values so that for each milestone year and location, one can see the increase in total average costs in relation to the amount of coverage one might receive from contracts with varying strikes. The cost increase is given by

$$Cost = 100*\frac{AVG(TotalCostsInsured)}{AVG(TotalCosts)} - 1 \tag{9}$$

where $AVG[TotalCostsInsured]$ is the average of the insured total costs and $AVG[TotalCosts]$ is the average of uninsured total costs. Contract loading, the percent by which the premium exceeds the expected payout or "actuarially fair price", is given by

$$Loading = 100*\frac{Premium(K)}{E[K]} - 1 \tag{10}$$

where $E[K]$ is the expected value of the payout function for a given strike K and $Premium(K)$ is the contract's relative price.

3.2.5. Contract evaluation

The risk metrics used to evaluate the performance of the contracts are reduction in cost semi-deviation and maximum cost savings over the 100-year simulated evaluation period. Semi-deviation is chosen because it is a common metric used to measure risk in investment decisions and can effectively quantify negative cash flow volatility. It is calculated as the standard deviation of yearly costs that lie above the yearly cost mean.

Maximum cost savings quantifies the savings the mine experiences during the worst solar year simulated, and is expressed as the percent reduction in costs between the maximum yearly energy expenditure of the mine with and without a contract, such that

$$MaxCostSavings = 100*\frac{MAX(TotalCosts)}{MAX(TotalCostsInsured)} - 1 \tag{11}$$

The maximum cost savings is used as a metric to address how the contract may act as a hedge against more extreme, less probable bad solar years.

4. Results & discussion

This chapter presents a discussion of the results of this study and is broken up into the following sections:

1. Developed contract: break-down of the indices developed for each contract and their respective basis risk analysis.
2. Contract performance: evaluation of contract ability to reduce cost semi-deviation, analysis of maximum total savings with contracts and analysis of physical risk mitigation influence.
3. Limitations & future work: description of limitations faced during study and what steps can be taken to further this research.

4.1. Developed contract

4.1.1. Developed index

The mine's total energy costs decrease with every progressive milestone year (2020–2050) for both locations, which is expected as the price of renewable technologies decreases. Focusing on the individual 300 simulations for each milestone year, costs fluctuations arise as a result of variations in operational costs, i.e. total energy imports, exports, and contract exceedances. Fixed-costs, representing investments in the energy system, see a large jump in 2025 as the optimization begins to select more renewable energies to install, thus forecasting that the influence of solar on the mine's energy expenditures significantly increases.

Energy imports are highly sensitive to monthly irradiance, particularly during winter when average daily irradiance drops. Cloud effects during summer months do not show significant effects on energy imports since consistently favorable sunny days occur and the energy system is able to generate and store enough energy to sustain the mine with minimal grid support. Sequences of the "Bad" cloudy day class also see a significant influence on costs, since these cloudy day streaks lead to exceptionally high imports

that trigger contract penalties.

In the year 2020, correlation between irradiance and total energy cost is negligible in both locations as the mine relies on the grid for energy imports. At location 1, only in year 2025 was the influence of solar significant enough to consider in this study (adjusted $R^2 = 0.32$). In milestone years 2030 and later the R^2 value fell below 0.2, suggesting that enough storage capacity is installed to mitigate any cloudy day effects. The correlation between irradiance and energy costs was much stronger in location 2 where cloud effects are more predominant, having significant R^2 values in all milestone years except for 2020. The regressions for each index, calculated using Equation (1), can be found in Table 2.

As can be seen in Table 2, every index regression took monthly winter irradiance sums, at both locations and for every milestone year, solidifying the role of these months as the key determiners in influencing cost variability. It can also be seen that sequences of the "Bad" cloudy days were significant in every regression as well. It is interesting that the significant variables do change in certain milestone years, for instance at location 2 year 2025, four day and six day sequences of "Excellent" cloudy days are considered, where only four day "Excellent" sequences are considered in other milestone years. The weight of each considered variable also changes slightly from year to year, suggesting that their influence do indeed change as PV-BESS technology gets cheaper and installed capacity increases, though these discrepancies are within each coefficient's standard error and can be considered negligible. Location 1 has a weaker index, only being influential for energy systems installed in 2025, while location 2 sees significant index influence for most years, especially after 2030 when the R^2 value hits 0.67. This discrepancy between the two locations shows the influence cloud effects can have, being predominant at location 2 but not location 1.

Comparing these index R^2 values with those from previous literature, the R^2 value for location 1 is low. As discussed in the methods section, observed coefficients of determination from other studies tend to be greater than 0.4, indicating the index at location 1 to be a poor indicator of energy expenditure.

4.1.2. Basis risk analysis

All the developed indices carry a certain amount of basis risk that defines the quality of each index. In Fig. 6, payouts triggered by the index are compared to actual damages experienced by the mine (damages refer to the payout corresponding to the actual total energy cost the mine experienced, see payout function Equation (2)) during the evaluation period for location 1 year 2025 and location 2 year 2050 are shown (strike set at the mean value of the index for each case). The index's predictive strength of total energy cost at location 1 is already significantly lower than at location 2 and is evident by the low correlation between payouts and actual damages ($R^2 = 0.24$). The relationship at location 2 is stronger, with an R^2 of 0.49, but this still indicates that there were a large amount

Table 2
Index regressions, where *I* signifies monthly total irradiance. *Bad*, *Good*, and *Exc* are the different yearly total cloudy day sequences according to class, where the subscript indicates the length of the sequence. E.g. Bad_2 refers to yearly total of "Bad" two day cloudy sequences. Note: Index regressions for Location 1 were only significant in milestone year 2025 ($R^2 < 0.2$ in other years, thus excluded from analysis).

Location/Year	Index Regression, S	Adjusted R^2
L1/2025	$563.33 - 9.43\times10^{-5}I_{\text{April}} - 1.38\times10^{-4}I_{\text{May}} - 7.85\times10^{-5}I_{\text{Jun}} - 1.63\times10^{-4}I_{\text{Jul}} + 3.11Bad_4 + 6.55Bad_5 - 0.38Good_5 - 0.32Good_6 - 1.35Good_{14} - 4.10Exc_{10}$	0.32
L2/2025	$793.62 - 1.10\times10^{-4}I_{\text{March}} - 9.84\times10^{-5}I_{\text{April}} - 1.70\times10^{-4}I_{\text{May}} - 2.86\times10^{-4}I_{\text{Jun}} - 2.54\times10^{-4}I_{\text{Jul}} - 1.25\times10^{-4}I_{\text{Aug}} - 1.07\times10^{-5}I_{\text{Sep}} - 1.10\times10^{-5}I_{\text{Oct}} + 0.57Bad_2 + 0.99Bad_3 + 2.58Bad_5 + 7.00Bad_6 + 7.61Bad_7 + 1.22Exc_4 - 2.78Exc_6$	0.60
L2/2030	$758.95 - 1.27\times10^{-4}I_{\text{March}} - 1.16\times10^{-4}I_{\text{April}} - 2.13\times10^{-4}I_{\text{May}} - 3.16\times10^{-4}I_{\text{Jun}} - 2.60\times10^{-4}I_{\text{Jul}} - 1.66\times10^{-4}I_{\text{Aug}} - 1.31\times10^{-5}I_{\text{Sep}} - 1.25\times10^{-5}I_{\text{Oct}} + 0.69Bad_2 + 1.06Bad_3 + 2.69Bad_5 + 6.51Bad_6 + 7.78Bad_7 - 2.81Exc_6$	0.67
L2/2035	$712.53 - 1.33\times10^{-4}I_{\text{March}} - 1.22\times10^{-4}I_{\text{April}} - 1.15\times10^{-4}I_{\text{May}} - 3.15\times10^{-4}I_{\text{Jun}} - 2.60\times10^{-4}I_{\text{Jul}} - 1.69\times10^{-4}I_{\text{Aug}} - 1.37\times10^{-5}I_{\text{Sep}} - 1.31\times10^{-5}I_{\text{Oct}} + 0.70Bad_2 + 1.07Bad_3 + 2.67Bad_5 + 6.43Bad_6 + 7.79Bad_7 - 2.83Exc_6$	0.67
L2/2040	$669.79 - 1.13\times10^{-4}I_{\text{March}} - 1.24\times10^{-4}I_{\text{April}} - 2.16\times10^{-4}I_{\text{May}} - I_{\text{Jun}} - 2.60\times10^{-4}I_{\text{Jul}} - 1.70\times10^{-4}I_{\text{Aug}} - 1.38\times10^{-5}I_{\text{Sep}} - 1.32\times10^{-5}I_{\text{Oct}} + 0.70Bad_2 + 1.07Bad_3 + 2.68Bad_5 + 6.43Bad_6 + 7.78Bad_7 - 2.83Exc_6$	0.67
L2/2045	$640.41 - 1.36\times10^{-4}I_{\text{March}} - 1.26\times10^{-4}I_{\text{April}} - 2.17\times10^{-4}I_{\text{May}} - I_{\text{Jun}} - 2.61\times10^{-4}I_{\text{Jul}} - 1.71\times10^{-4}I_{\text{Aug}} - 1.40\times10^{-5}I_{\text{Sep}} - 1.34\times10^{-5}I_{\text{Oct}} + 0.71Bad_2 + 1.08Bad_3 + 2.69Bad_5 + 6.45Bad_6 + 7.78Bad_7 - 2.82Exc_6$	0.67
L2/2050	$619.80 - 1.37\times10^{-4}I_{\text{March}} - 1.28\times10^{-4}I_{\text{April}} - 2.18\times10^{-4}I_{\text{May}} - I_{\text{Jun}} - 2.62\times10^{-4}I_{\text{Jul}} - 1.73\times10^{-4}I_{\text{Aug}} - 1.42\times10^{-5}I_{\text{Sep}} - 1.35\times10^{-5}I_{\text{Oct}} + 0.71Bad_2 + 1.08Bad_3 + 2.69Bad_5 + 6.46Bad_6 + 7.77Bad_7 - 2.81Exc_6$	0.67

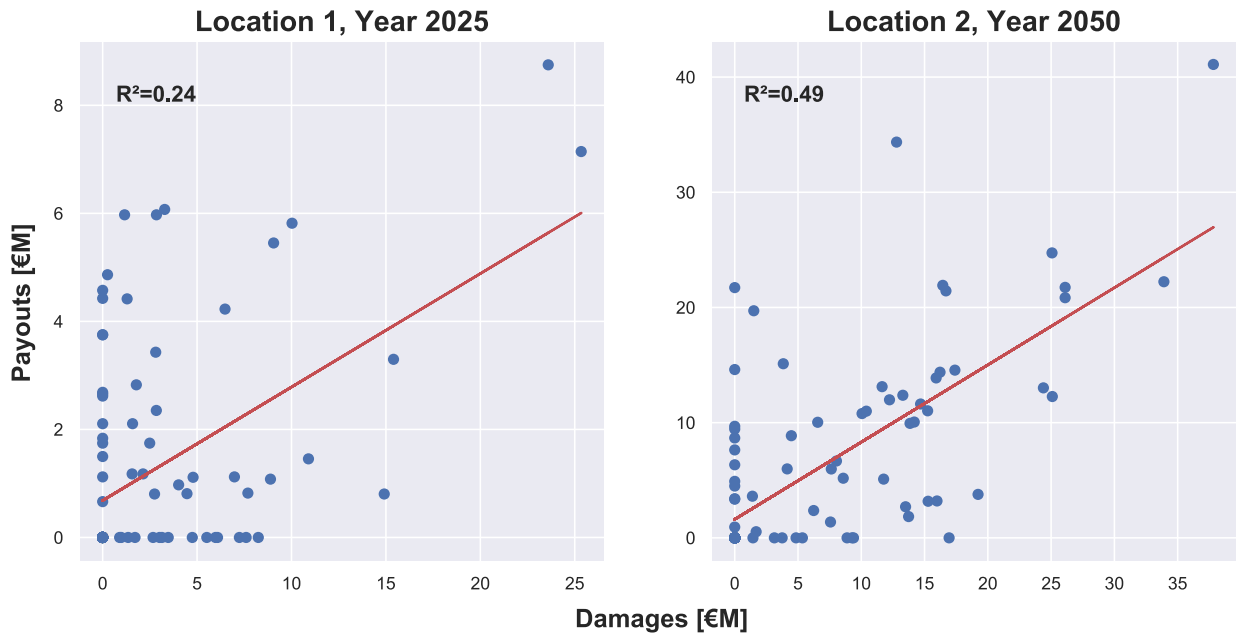

Fig. 6. Correlation between actual damages and payout made according to index, where damages refer to payout corresponding to the actual total energy cost the mine experienced. Figures shown for locations 1 and 2 for the years 2025 and 2050 with a strike set at the average index value.

of "misses". In both cases, there were instances where the registered payout was zero, yet damages were quite substantial, greater than €15 million (about 4% of average total costs) at one point. There were also instances where the mine did receive a payout yet experienced no damages, less problematic for the mine but indicating inaccuracy in the index.

The payout vs. actual damage graphic is also presented in Refs. [39], where various types of indices for hedging hydropower hydrologic risk considering natural gas price uncertainty were analyzed. In the case of that study, correlation between payouts and damages dropped to $R^2 = 0.42$, exhibiting similar behavior of the "misses" seen in Fig. 6. The "misses" with regard to the present paper indicate moments where the mine energy demand spiked and the index measured corresponded to above average irradiance, or when the demand dropped and the index measured corresponded to below average irradiance. Both situations cause either an unjustified payout or reimbursed damage.

4.2. Contract performance

4.2.1. Reduction in cash flow volatility

All the selected cases (one year at location 1, six different years at location 2) of this study have been plotted together for each evaluation metric against the expected increase in total cost. The expected increase in total cost follows strike value decreases between the 100th and 50th percentile of the index distribution and can effectively show at what cost the mine can achieve the relative risk mitigation quantity. This method allows for a visually intuitive way for a potential contract buyer to know what they essentially are buying.

The first metric is total cost semi-deviation reduction and both locations see large potential reductions (Fig. 7). Location 1 sees a reduction of 17.5% for an increased total cost of 0.35%, though this can be skewed due to the small amount of extremely high costs experienced during the simulation. The expected increase in total cost nearly matches that of the reduction in deviation, therefore hinting that cash flow volatility reduction might not be the best metric for measuring the effectiveness of the contract at location 1.

Location 2 shows more promising results. Semi-deviation reductions reach 32% for increases in total cost of less than 0.5%. Installations of energy systems in year 2025 experience the smallest reduction in volatility for comparably similar cost increases for installations in later years due to less installed energy system infrastructure and greater dependency on the grid. There is also an apparent limit in contract effectiveness at around a 0.1% total cost increase as the curve completely flattens out. It seems that contracts taking on strikes at the 75th percentile of the index distribution result in the most economic risk mitigation. Years 2040 through 2050 see a reduction in contract effectiveness as they pay more for less risk mitigation. At this point *physical risk mitigation* via increases in energy storage investment begin to reduce the utility of a the *financial risk mitigation* measure. The year that benefits the most from the contracts is 2030, when the mine's dependency on its energy system is fairly substantial but due to high storage costs cannot economically bridge long cloudy day sequences. Thus contracts are most suitable for energy system installations implemented at this time and can act as a risk mitigation measure during the transition period to fully renewable energy systems. It's worth noting the discontinuous behavior of the plots, indicators of basis risk when the indices could not correctly categorize the solar year. Similar behavior is seen in [39].

A helpful way to visualize how cost deviation is reduced is by plotting the relative total costs of the 100 years of simulated evaluation data with and without a contract at varying strike values. Fig. 8 shows series for energy systems installed in both locations in the year 2025 for two different strikes, one set at the average index (essentially hedging loss from all sub-average years) and the other set at one standard deviation above the index mean. The horizontal line indicates the average annual energy cost, while values above the line indicate higher cost years and values below the line represent lower cost years. One can see the effect of the contracts as the reduce the overall deviation in costs, trimming in particular the peaks.

At location 1, cost deviation reduces more noticeably with the

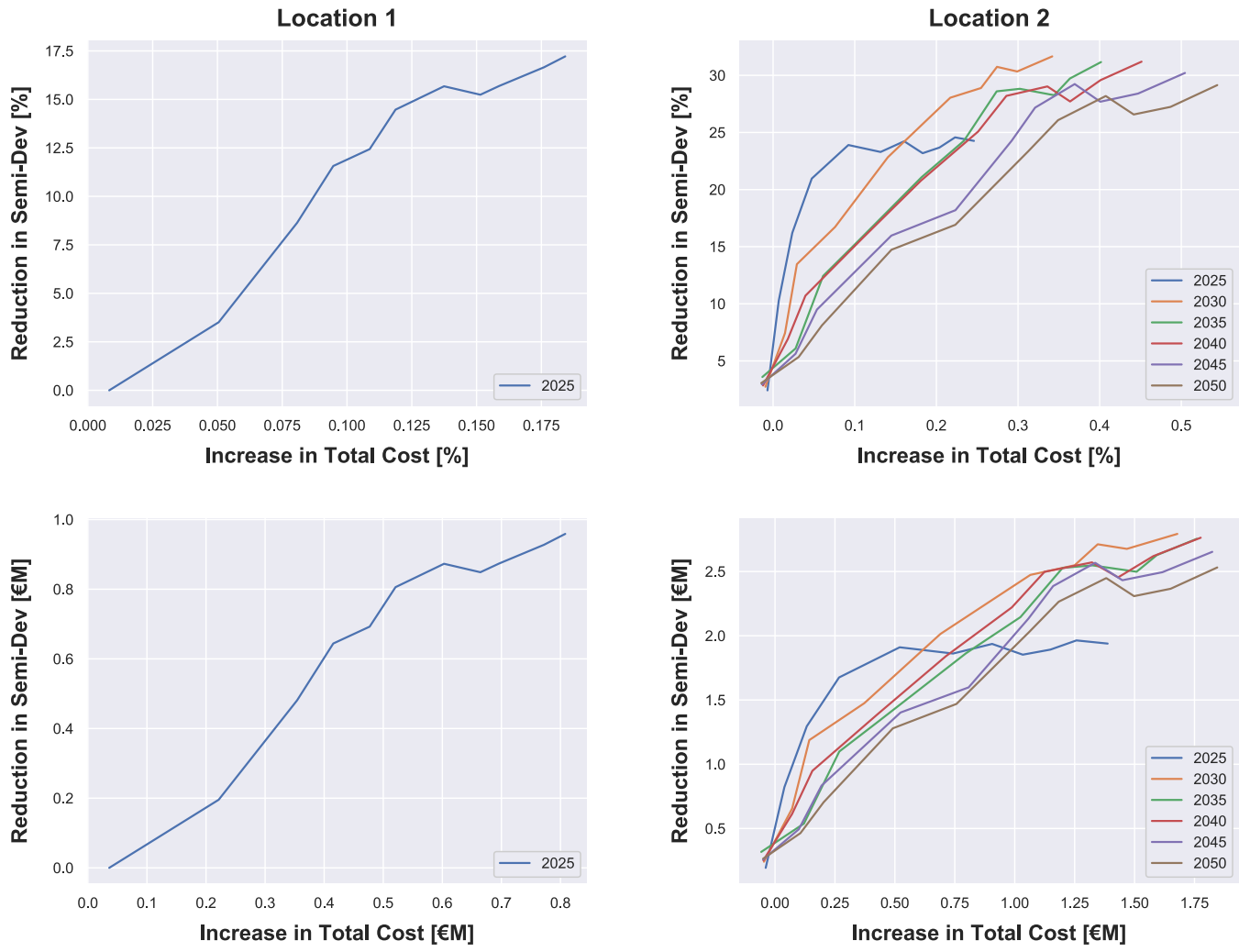

Fig. 7. Reduction in total cost semi-deviation seen during evaluation period. Discontinuous behavior of the plots indicates basis risk when the indices could not correctly categorize the solar year. Similar behavior is seen in Ref. [39].

smaller strike value (strike set at mean cost), and cost reductions are experienced primarily at peaks, indicating that average years are more heavily influenced by variation in the mine's demand (rock hardness in the mine feed) rather than cloud effects (as evidenced by the low index R^2 at location 1). Location 2 sees an overall greater reduction in deviation in costs, indicating a stronger ability to hedge risk for both cost peaks and average years.

To summarize, reductions in total cost semi-deviation are relatively large for both locations, though they are substantially larger at location 2, especially in year 2030. Thus it might be worth continuing research into these contracts for cloudier climates. Since the estimated increase in average costs at location 1 is about equal to the reductions in semi-deviation, and contracts are only significant for installations made in year 2025, the utility and relevance of a weather derivative contract for cash flow volatility reduction might not be an attractive solution for mines in high irradiance regions. In Ref. [3], a revision of the results in cash flow volatility reduction of various agricultural weather derivative papers is presented, showing reductions in semi-variance between 16 and 77%, indicating the volatility reductions in this paper sit within the range of observed results from similar research.

4.2.2. *Maximum cost savings during poorest solar years*

The second metric is maximum total cost savings and addresses the maximum savings the mine experienced during the simulated evaluation years, defined as the percent difference in maximum total cost with and without a contract (see Equation (11)). These results are shown in Fig. 9.

At location 1 the mine can save up to 1.2% of its costs in any given year, or roughly €5 million. This comes at an average cost increase of 0.35%. This metric gives a better picture of the hedging potential of a contract at location 1 and can be useful for mines operating with limited emergency funds. One can see this referring back to Fig. 8, where the greatest cost reductions for locations 1 occur at peaks.

Location 2 exhibits very promising behavior in regards to hedging extremely poor solar years. For increases of less than 0.5% in total costs, maximum savings approach 3.5%. In the case of year 2035, the mine could see a savings of nearly 3.25% (about €14.5 million) for an average cost increase of 0.35% (€1.25 million). Once again year 2025 sees the smallest impact from the contract while energy system installations made in year 2030 see the most benefit from a contract. Years 2045 and 2050 do have the greatest savings as a percent of total cost, though the total costs are substantially

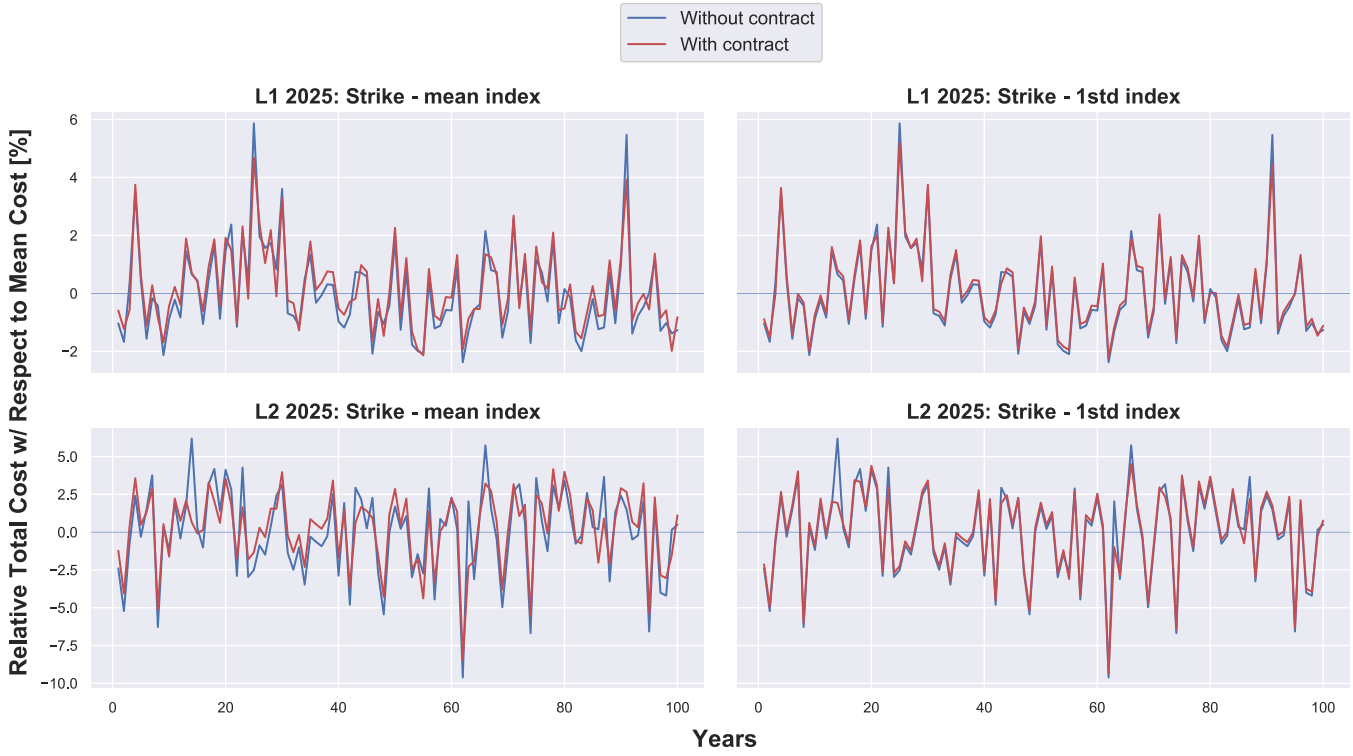

Fig. 8. Simulations of mine operations with and without contracts at different strikes. Y axis shows relative total annual energy cost with respect to average energy cost, indicated with horizontal line at y = 0. Values above zero indicate higher cost years while values below zero indicate lower cost years.

lower during these later years.

To summarize, at location 1, the use of a weather derivative to hedge the poorest of solar years might be more attractive than using it for hedging cost volatility, since savings can reach €5 million in any given year. But this again is only possible for installations in year 2025 and thus restricted. Location 2 once again shows a lot more potential for maximum cost savings in years 2025 forward.

4.2.3. Financial vs. physical risk mitigation

The mitigation ability of the contracts changes in each milestone year due to influence of physical risk mitigation measures (storage systems) also at play in the optimization model. The general behavior is the contracts require the mine to depend partially on the energy system to have any effect, but as costs for the physical mitigation measures decrease and more can be installed, the weather derivative's mitigation ability decreases. This is observed in Fig. 10 (left side) where the average reduction in total cost semi-deviation for a contract costing an average of 0.2% of total costs is plotted for each milestone year. There is a jump from 2025 to 2030, when the contact behaves optimally, then a dramatic decrease in effectiveness occurs until 2050. Jumps between plateaus of mitigation ability, as seen from 2030 to 2035 and 2040 to 2045, indicate key years when energy storage costs have lots of influence on contract value.

Also incorporated in the optimization model are the size of the mine's power contract (GW), which drops significantly from 2025 to 2030, then goes to zero from 2035 on, and the contract exceedance amount (GW), which jumps from 2025 to 2030 and then gradually increases in the proceeding years.

To determine which physical and/or contractual component of the energy system had the greatest influence on the hedging ability of the weather derivative, correlations between the reduction in semi-deviation for contracts of 0.2% of total costs and each component were determined for years 2030–2050, shown in Table 3.

All components had an effect on the contract hedging ability, but the effect of installing more batteries has the greatest effect, showing very strong negative correlations with semi-deviation cost reduction. Capacity increase in the battery converter is seen to have an almost perfect negative correlation with contract effectiveness. The relationship between battery converter capacity and contract semi-deviation cost reduction is shown in Fig. 10 (right side).

4.3. Limitations & future work

It is worth mentioning the validity of these results is dependent on the mine energy management model used to generate the yearly energy costs. This model takes into account SAG mill hourly power load and not power loads from other mine operations, and though the results in this study refer to all energy costs as total energy costs, they specifically address the SAG mill energy demand. The SAG mill is the largest electricity consumer of the mining process, thus it is a good estimation of the mines total electricity demand, but for future studies, a more comprehensive energy demand input should be deployed for capturing the other energy vectors.

Two different climates were analyzed in this study, an arid climate and a Mediterranean climate. It would be worth investigating contract effectiveness in additional climates.

Energy storage technology inputs into the model included battery energy storage and power-to-gas. The results of this study could differ significantly if other physical risk mitigation measures are incorporated as inputs to the model.

The contract structure used in this study was a call option, though other contract structures exist that could be applied to the contracts developed in this paper.

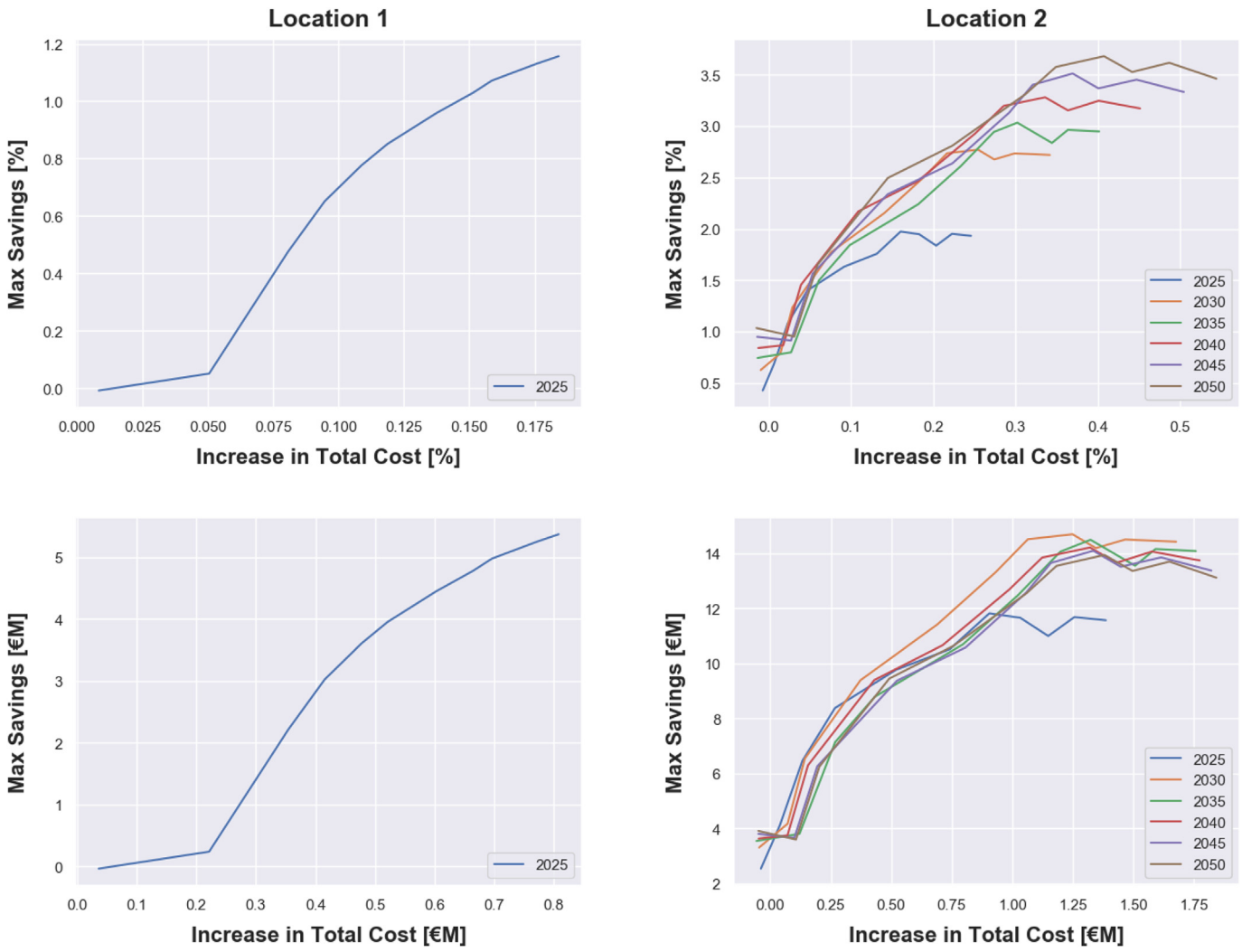

Fig. 9. Maximum savings seen during evaluation period.

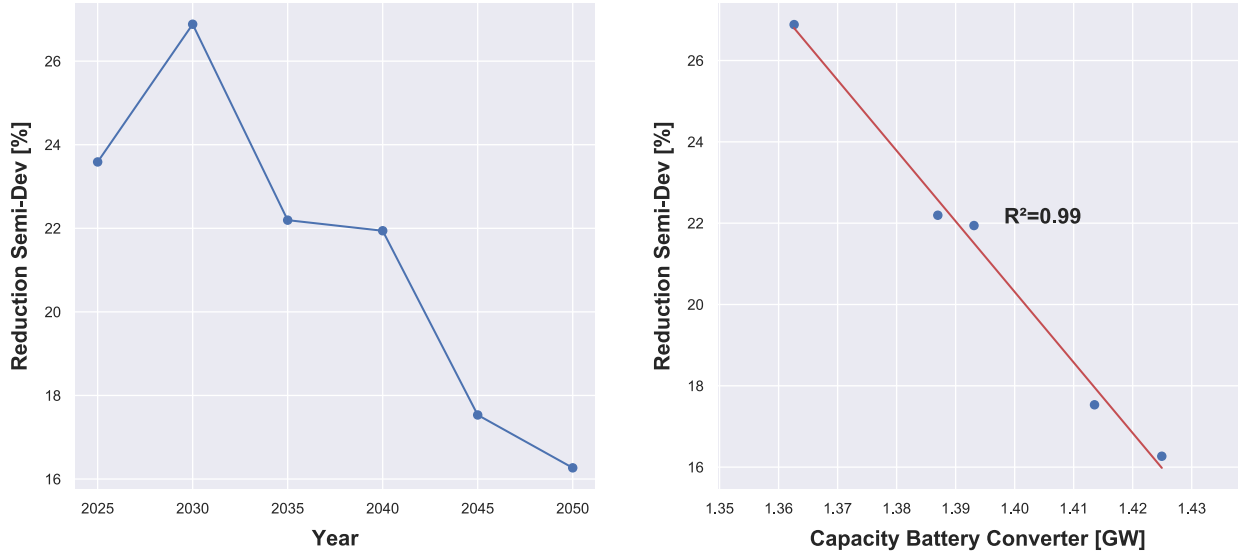

Fig. 10. Left: Reduction in total cost semi-deviation with contract for an average increase of total costs of 0.2% for each milestone year. Right: Relationship between reductions in semi-deviation with contract for average increase in total cost of 0.2% and capacity of battery converter installed.

Table 3
Correlations between physical/contractual risk mitigation measures and the financial weather derivative mitigation measure.

Component	r	R^2
	0.69	0.47
Solar PV (GW)		
Battery Converter (GW)	−0.99	0.99
Battery Storage Size (GWh)	−0.98	0.97
Power-to-Gas Converter (GW)	−0.59	0.35
Power-to-Gas Storage Size (GWh)	−0.94	0.90
Contract Size (GW)	0.78	0.61
Contract Exceedance (GW)	−0.91	0.83

These contracts were applied specifically to a mining scheme in Chile where energy costs are dependent on energy imports, exports and power contract penalties. It would be interesting to apply the same methodology used in this paper to develop an irradiance-based weather derivative for another industry with different energy cost sources and energy profiles.

The models used for index prediction were multiple linear regressions. Even though correlations between solar irradiance and energy cost are believed to be representative, more sophisticated models could be developed to improve the correlation between the independent and dependent variables. This study used monthly sum irradiance and cloudy day sequencing as the basis of the indices developed. Other variables such as temperature could also be incorporated into the indices in order to improve predictive power. With the proliferation of solar technologies around the globe, there will undoubtedly be a greater need to study solar effects on solar user energy financing.

5. Conclusion

Index-based financial contracts have been used in various sectors to provide coverage against weather-related financial risk. The goal of this study is to extend the concept of index-based weather derivative contracts to act as a hedge against solar variability by developing an irradiance-based index. To analyze the efficacy of the index, contracts were applied to Chilean mines installing commercial size PV arrays. The contracts' effectiveness was determined by their ability to reduce the mines' financial risk due to solar volatility (due to sequences of cloudy days).

This research used a linear optimization model called LEELO that determined optimal sizes of a solar, battery, and power-to-gas systems, as well as power contract size, component operation schedule, and total annual energy cost for a mine. The inputs to the model were series of hourly mine power demand and hourly available irradiance profiles, both subject to Monte-Carlo randomization. The indices for the weather derivative contracts were developed by correlating the solar input profiles with total annual energy costs. This was done by means of regression analysis using predictive variables of monthly irradiance and cloudy day sequencing. The contract lengths were set at one year and the payment structure took the form of a call option. The contracts were evaluated comparing total annual mine energy costs with and without a contract in place. To test the effect different climates have on the contracts, two different climatic locations were evaluated. To analyze the influence of decreasing costs of PV and energy storage technology throughout time, the model was run for both locations for six milestone-years between 2020–2050.

Results from the evaluation period show that the designed contracts can effectively reduce mine cash flow volatility and increase savings during the poorest of solar years. Cash flow volatility is reduced up to 17.5%, coming at an average total cost increase of less than 0.35% at location 1. A semi-deviation reduction of 32% with 0.5% cost increase was observed at location 2. During the evaluation period, location 1 saw a maximum annual saving of 1.2% for average total cost increase of 0.35%, and location 2 a maximum annual saving of 3.5% for 0.5% average total cost increase.

The efficacy of the contracts are very climate dependent. The influence of cloud effects were much stronger at the second location selected in this study, located in central Chile in a Mediterranean climate. Location 1, located in the northern Atacama region, is very arid and experiences little cloud activity influential enough to affect energy costs. The excellent solar levels witnessed in this region make the designed energy system robust, not needing weather insurance. This can be seen in the R^2 values correlating the indices developed at each location with annual mine energy expenditures, which ranged from 0.6 to 0.67 at location 2 for the various milestone years between 2025–2050, and 0.32 for the milestone year 2025 at location 2.

For both locations the contracts show no utility before 2025 since the mine is predominantly reliant on energy imports. At location 1, contracts are only effective for systems installed in 2025. In later years, mines can economically install enough storage capacity to cope with cloudy periods. Contracts at location 2 are effective for all systems installed after 2025, though their greatest potential is seen for systems built in 2030. The attractiveness of contracts drops after 2030 as cheap energy storage, particularly batteries, emerges as a physical risk mitigation option.

This work acts as a first step toward realizing irradiance-based weather derivatives and sets a framework for how to develop them. It specifically addresses commercial solar systems in the context of Chilean mining, though its framework can be and is encouraged to be applied to other sectors of the solar industry.

CRediT authorship contribution statement

Colin F.H. Boyle: Methodology, Formal analysis, Investigation, Writing - original draft, Visualization. **Jannik Haas:** Conceptualization, Resources, Supervision, Writing - review & editing. **Jordan D. Kern:** Methodology, Supervision, Writing - review & editing.

Declaration of competing interest

The authors declare that they have no known competing financial interests or personal relationships that could have appeared to influence the work reported in this paper.

Acknowledgments

We appreciate the support of the German Research Foundation [DFG-NO 805/11-1] and the Chilean National Agency for Research and Development [ANID/FONDAP/15110019].

References

[1] U.S. Global Change Research Program, National climate assessment, extreme weather. https://nca2014.globalchange.gov/highlights/report-findings/extreme-weather, 2014. Last accessed on 2019-12-12.
[2] B. Finas, The transfer of weather risk faced with the challenges of the future, Techn. Newslett. (2012). URL https://agroinsurance.com/files/documents/pc_nl_cata_naturelles_en.pdf.
[3] I. Stulec, K. Petljak, T. Bakovic, Effectiveness of weather derivatives as a hedge against the weather risk in agriculture, Agric. Econ. – Czech 62 (2016) 356–362.
[4] International Energy Agency (IEA), Renewables 2019, IEA, Paris, 2019, 2019. URL, renewables2019.
[5] Felix Cebulla, Jannik Haas, Joshua Eichman, Wolfgang Nowak, Pierluigi Mancarella, How Much Electrical Energy Storage Do We Need? A Synthesis for the U.S., Europe, and Germany, 181, Journal of Cleaner Production, 2018.

[6] Haas, J., Cebulla, F., Cao KK., Nowak W., Palma-Behnke R., Rahman C., Mancarella P. Challenges and trends of energy storage expansion planning for flexibility provision in low-carbon power systems - a review, Renew. Sustain. Energy Rev. 80. 2018 doi:10.1016/j.rser.2017.05.201. URL http://gen.lib.rus.ec/scimag/index.php?s=10.1016/j.rser.2017.05.201.
[7] Juan Ocaranza. Anuario de Estadísticas del Cobre y Otros Minerales (Yearbook: Copper and Other Mineral Statistics), COCHILCO, 2020.
[8] F. Cambero, Floating solar panels to boost efficiency at Chilean copper mine, URL, https://www.reuters.com/article/us-chile-mining-solar/floating-solar-panels-to-boost-efficiency-at-chilean-copper-mine-idUSKCN1QV2IZ.
[9] A. Müller, M. Grandi, Weather derivatives: a risk management tool for weather-sensitive industries, Geneva Pap. Risk Insur. - Issues Pract. 25 (2) (2000) 273–287, https://doi.org/10.1111/1468-0440.00065, 10.1111/1468-0440.00065. URL.
[10] J. Cogen, What is weather risk? pMA OnLine Magazine, 1998. URL, http://www.retailenergy.com/articles/weather/htm.
[11] C.-H.H. Tang, S.S. Jang, Weather risk management in ski resorts: financial hedging and geographical diversification, Int. J. Hospit. Manag. 30 (2) (2011) 301–311, https://doi.org/10.1016/j.ijhm.2010.09.012. URL http://www.sciencedirect.com/science/article/pii/S0278431910001258.
[12] P. Brockett, M. Wang, C. Yang, Weather derivatives and weather risk management, Risk Manag. Insur. Rev. 8 (2005), https://doi.org/10.1111/j.1540-6296.2005.00052.x.
[13] I. Stulec, Effectiveness of weather derivatives as a risk management tool in food retail: the case of Croatia, Fin, Stud 5 (2) (2017).
[14] Li, Anlong and Cao, Melanie and Wei, Jason Zhanshun, Precipitation Modeling and Contract Valuation: A Frontier in Weather Derivatives. Journal of Alternative Investments, Vol. 7, No. 2, 2004, Available at SSRN: https://ssrn.com/abstract=1016137.
[15] T. Markovic, C. Husemann, S. Ivanovic, V. Zekic, Drought insurance in wheat and corn production with weather derivatives: the case of Serbia, Custos e Agronegocio 11 (2015) 189–202.
[16] DV Vedenov, Barry Barnett, Efficiency of weather derivatives as primary crop insurance instruments, Western journal of agricultural economics 29 (2004) 387–403.
[17] A. Alexandridis, A. Zapranis, Wind derivatives: modeling and pricing, Comput. Econ. 43 (3) (2013) 299–326.
[18] C. Richard, Weather-risk hedge used at new enel project, Wind Power Monthly, 7 Jan. 2019, https://www.windpowermonthly.com/article/1522160/weather-risk-hedge-used-new-enel-project. Accessed 10 Oct. 2020.
[19] Bhattacharya, Saptarshi & Gupta, Aparna & Kar, Koushik & Owusu, Abena. (2015). Hedging strategies for risk reduction through weather derivatives in renewable energy markets. 1190-1195. 10.1109/ICRERA.2015.7418597.
[20] T. Matsumoto, Y. YamadaCross, Hedging Using Prediction Error Weather Derivatives for Loss of Solar Output Prediction Errors in Electricity Market. Asia-Pac Financ Markets 26 (2019) 211–227. https://doi.org/10.1007/s10690-018-9264-3.
[21] D. Kahan, Food A.O. of the United Nations, Managing Risk in Farming, Farm Management Extension Guide, Food and Agriculture Organization of the United Nations, 2013. URL https://books.google.de/books?id=QSfxmwEACAAJ.
[22] B.T. Foster, J.D. Kern, G.W. Characklis, Mitigating hydrologic financial risk in hydropower generation using index-based financial instruments, Water Resourc. Econ. 10 (2015) 45–67, https://doi.org/10.1016/j.wre.2015.04.001. URL http://www.sciencedirect.com/science/article/pii/S2212428415000146.
[23] D. Torriani, P. Calanca, M. Beniston, J. Fuhrer, Hedging with weather derivatives to cope with climate variability and change in grain maize production, Agric. Finance Rev. 68 (2008) 67–81, https://doi.org/10.1108/00214660880001219.
[24] Jannik Haas, Felix Cebulla, Wolfgang Nowak, Claudia Rahman, Rodrigo Palma-Behnke, A multi-service approach for planning the optimal mix of energy storage technologies in a fully-renewable power supply, Energy Convers. Manag. 178 (2018) 355–368, https://doi.org/10.1016/j.enconman.2018.09.087. URL, http://www.sciencedirect.com/science/article/pii/S0196890418310987.
[25] G. Pamparana, W. Kracht, J. Haas, J. Ortiz, W. Nowak, R. Palma-Behnke, Studying the integration of solar energy into the operation of a semi-autogenous grinding mill. part i: framework, model development and effect of solar irradiance forecasting, Miner. Eng. 137 (2019) 68–77, https://doi.org/10.1016/j.mineng.2019.03.017.
[26] G. Pamparana, W. Kracht, J. Haas, J. Ortiz, W. Nowak, R. Palma-Behnke, Studying the integration of solar energy into the operation of a semi-autogenous grinding mill. part ii: effect of ore hardness variability, geometallurgical modeling and demand side management, Miner. Eng. 137 (2019) 53–67, https://doi.org/10.1016/j.mineng.2019.03.016. URL, http://www.sciencedirect.com/science/article/pii/S0892687519301426.
[27] M. Lambert, Power-to-gas: linking electricity and gas in a decarbonising world?, Oxford Instit, Energy Stud., Oxford Energy Insight 39 (2018).
[28] M. Child, C. Breyer, D. Bogdanov, H.-J. Fell, The role of storage technologies for the transition to a 100% renewable energy system in Ukraine, Energy Procedia 135 (2017) 410–423, https://doi.org/10.1016/j.egypro.2017.09.513, 11th International Renewable Energy Storage Conference, IRES 2017, 14-16 March 2017, Düsseldorf, Germany, URL, http://www.sciencedirect.com/science/article/pii/S1876610217346180.
[29] A. Molina, M. Falvey, R. Rondanelli, A solar radiation database for Chile, Sci Rep 7 (2017) 14823. https://doi.org/10.1038/s41598-017-13761-x.
[30] P. Alaton, B. Djehiche, D. Stillberger, On modelling and pricing weather derivatives, Appl. Math. Finance 9 (1) (2002) 1–20. URL, https://EconPapers.repec.org/RePEc:taf:apmtfi:v:9:y:2002:i:1:p:1-20.
[31] M. Miranda, D.V. Vedenov, Innovations in agricultural and natural disaster insurance, Am. J. Agric. Econ. 83 (3) (2001) 650–655. URL, http://www.jstor.org/stable/1245094.
[32] N. Jensen, C. Barrett, A. Mude, Index insurance quality and basis risk: evidence from northern Kenya, Am. J. Agric. Econ. 98 (2016), aaw046, https://doi.org/10.1093/ajae/aaw046.
[33] Turvey, Calum G. "Weather Derivatives for Specific Event Risks in Agriculture." *Review of Agricultural Economics*, vol. 23, no. 2, 2001, pp. 333–351. *JSTOR*, www.jstor.org/stable/1349952.
[34] P. Barrieu, O. Scaillet, A Primer on Weather Derivatives, Springer, Boston, MA, 2009.
[35] T.J. Richards, Mark R. Manfredo, Dwight R. Sanders, Pricing Weather Derivatives, Morrison School of Agribusiness and Resource Management, Faculty Working Paper Series, SSNR, 2004.
[36] Stephen Jewson, Brix Anders, Christine Ziehmann, Weather Derivative Valuation: the Meteorological, Statistical, Financial and Mathematical Foundations, Cambridge University Press, 2005.
[37] S.S. Wang, A class of distortion operators for pricing financial and insurance risks, J. Risk Insur. 67 (1) (2000) 15–36. URL http://www.jstor.org/stable/253675.
[38] S. Wang, A Universal Framework for Pricing Financial and Insurance Risks, ASTIN Bulletin 32 (2) (2002) 213–234, https://doi.org/10.2143/AST.32.2.1027.
[39] J.D. Kern, G.W. Characklis, B.T. Foster, Natural gas price uncertainty and the cost-effectiveness of hedging against low hydropower revenues caused by drought, Water Resour. Res. 51 (4) (2015) 2412–2427, https://doi.org/10.1002/2014WR016533.